

Electrooxidation of Nitrite Ions on Gold/Polyaniline/Carbon Paste Electrode

Mohammad Etesami^{1,2,*}, Nurul S. N. M. S. Chandran², M. Hazwan Hussin², Adnan Ripin^{1,3}, Rohana Adnan², Amat Ngilmi A. Sujari², Norita Mohamed^{2,*}

¹ Advanced Materials Research Group, Institute of Hydrogen Energy, Universiti Teknologi Malaysia, 54100 Kuala Lumpur, Malaysia

² School of Chemical Sciences, Universiti Sains Malaysia, 11800 Minden, Penang, Malaysia

³ Faculty of Chemical Engineering, Universiti Teknologi Malaysia, 81310 UTM Johor Bahru, Johor, Malaysia

*E-mail: md.etesami@gmail.com, mnorita@usm.my

Received: 12 April 2016 / Accepted: 11 June 2016 / Published: 6 September 2016

Nitrite ions can penetrate from fertilizers into underground water and consequently contaminate the water and food sources. A facile two-step electrochemical method was used to fabricate gold/polyaniline/carbon paste electrode (Au/PAni/CPE) for nitrite sensing. The Au/PAni/CPE was visualized and characterized by scanning electron microscopy, energy-dispersed X-ray spectroscopy, X-ray diffraction and electrochemical methods. The electrocatalytic activity of bare CPE, PAni/CPE and Au/PAni/CPE toward the electrooxidation of nitrite was examined and compared via cyclic voltammetry. To obtain the optimal condition for fabrication of the electrode, the number of cycles in cyclic voltammetry for synthesis of polyaniline and the deposition time in potentiostatic deposition of gold were optimized with respect to the electrooxidation of nitrite. In a phosphate buffer solution (PBS, pH 7.0), the peak current was linear to the concentration of nitrite in the range from 3.8×10^{-5} M to 1.0×10^{-3} M with a detection limit of 2.5×10^{-5} M. The interference effect on the nitrite detection was also studied. The proposed method was also employed for the determination of nitrite in rain and lake water samples.

Keywords: Nitrite, Carbon paste electrode, Polyaniline, Gold particles, Electrocatalysis

1. INTRODUCTION

Nitrites can be extensively found in the environment as fertilizers, and in food products as additives and preservatives [1]. Nitrites can enter the environment and pollute the soil and water. Excess of nitrite can be poisonous to animals and human beings by forming the carcinogenic nitrosamines which cause a fatal disease, methaemoglobinaemia. Therefore, an accurate, rapid and

simple quantitative analysis of nitrite is essential to ensure high quality food and drinking water, public health and environmental protection.

Numerous methods have been developed for the determination of nitrite, such as spectrophotometry [2-4], ion chromatography [5, 6], high performance liquid chromatography [7, 8], gas chromatography [9], capillary electrophoresis [10, 11], and electrochemical methods [12-15]. Electrochemical methods have been widely used due to their convenience, cost-effectiveness, rapidness and simplicity. Nitrite can be electrochemically studied via oxidation or reduction processes at bare or modified electrodes. Study of nitrite via electrooxidation excludes the concern for dissolved oxygen as interference [16-18].

Electrochemical determination of nitrite has been reported at bare and modified electrodes, such as glassy carbon electrode (GCE) [14], diamond [19], palladium [20], silver [21], platinum [22, 23], gold [24], copper and transition metal oxide electrodes or catalysts [25]. Carbon paste electrodes (CPEs), which are made up of a homogeneous mixture of a carbon material and an organic liquid oil, have been used for electrochemical analysis due to their wide potential window, easily renewable surface, simplicity in fabrication, portability, high sensitivity in sensing and cost-effectiveness [26]. However, the application of bare electrodes are limited because of the electrode surface poisoning from several species and high overpotential in direct electroreduction/electrooxidation of nitrite ions [17]. Hence chemically modified carbon paste electrodes (CPEs) have been used with improved properties such as sensitivity, selectivity, detection limit, etc [27-30].

In recent years, noble metal nanostructured materials have attracted much attention in electrocatalysis. Gold nanoparticles (GNPs) modified electrodes present larger surface area and more active sites for the electrooxidation or electroreduction processes compared to unmodified electrodes and subsequently improve the detection limit, sensitivity and response potential window in electrochemical studies [31-35]. Moreover, the application of gold particles modified electrode compared to the gold electrodes is preferred in case of expense, renewability and catalytic properties in electrooxidation of nitrite.

Conducting polymers such as polyaniline (PAni) and polypyrrole (Ppy) have a wide applications as electrode materials and have been used in nitrite detection and bioelectrocatalytic determination of nitrite [36-38]. Among conducting polymers, PAni and Ppy have intriguing electronic and electrochemical properties for sensor applications. These synthesized polymers are uniform, homogeneous and facile to synthesize as well as possessing high electronic conduction and good environmental stability [39, 40]. Incorporating metal particles on/into the polymer modified electrodes results in the dispersion of metal particles in the polymer and consequently improves the electrocatalytic activity for nitrite oxidation by offering a larger specific surface area and enriching reactive sites [36].

The aim of this study is to fabricate a simple gold particles/polyaniline modified carbon paste electrode (Au/PAni/CPE) by electrochemical methods to study the electrocatalytic oxidation of nitrite and compare the electrocatalytic performance of the bare and modified electrodes. The factors affecting the nitrite electrooxidation are also studied after surface characterization of the prepared electrodes.

2. EXPERIMENTAL

2.1. Chemicals and Apparatus

NaAuCl₄ (99.999%) and Aniline (99.5%) were purchased from Sigma-Aldrich. All other chemicals and reagents used were of analytical grade. All chemicals used without further purification. All solutions were prepared using distilled water (18 MΩ cm). A phosphate buffer solution (0.10 M PBS, pH 7.0) was used as the supporting electrolyte. Insulin syringes (0.50 mL) were purchased from a local pharmaceutical store. The surface morphology of the bare and modified electrodes was characterized by a scanning electron microscope (Leo Supra 50 VP) equipped with energy dispersive X-ray spectrometer (EDX). An eDAQ EA 161 potentiostat connected to e-corder 410 (4-channel recorder) equipped by EChem software v2.1.0 were used for the electrochemical experiments. A conventional three-electrode electrochemical cell was used for the cyclic voltammetry and chronoamperometry where an Ag/AgCl (sat. KCl), a platinum wire and a bare/modified CPE were used as the reference, auxiliary and working electrodes, respectively. Electrochemical impedance spectroscopy (EIS) was conducted under AC voltage amplitude of 5mV in the frequency range of 100 kHz to 0.10 Hz using Gamry Reference 600.

2.2. Preparation of Modified CPE

The carbon paste electrode (CPE) was prepared by hand mixing of graphite powder with paraffin oil (70:30 w/w) in an agate mortar with pestle. The homogeneous paste mixture was inserted into the insulin syringe tip (i.d. 2 mm). The carbon paste was compressed into the tube to ensure that no air was trapped inside the tube. A copper wire was introduced to the compacted paste for electrical connection.

Polyaniline (PAni) film was deposited on the surface of carbon paste by repeatedly sweeping potential between -0.20 V and +0.80 V for a number of cycles at a scan rate of 50 mV s⁻¹ in an aqueous solution of 1.0 M HCl containing 0.10 M aniline. The thickness of the polymer film is then calculated.

The Au/PAni/CPE was prepared by immersing PANI/CPE into a 0.20 M H₂SO₄ containing 5 mM NaAuCl₄. A constant potential of -0.2 V was applied for several minutes. Then, the modified electrode was washed with distilled water and dried carefully. All solutions were purged by bubbling oxygen free nitrogen for 20 min.

3. RESULTS AND DISCUSSION

3.1. Electrodeposition of PANI and Au Particles

The cyclic voltammograms of formation of PAni on the CPE are shown in Figure 1a. To obtain the optimum number of cycles of PAni electropolymerization, the PAni/CPE electrodes with different

amounts of PANi were prepared and the electrocatalytic performance of the PANi/CPE electrodes were evaluated in a 0.10 M PBS 7 + 0.50 mM nitrite solution by cyclic voltammetry.

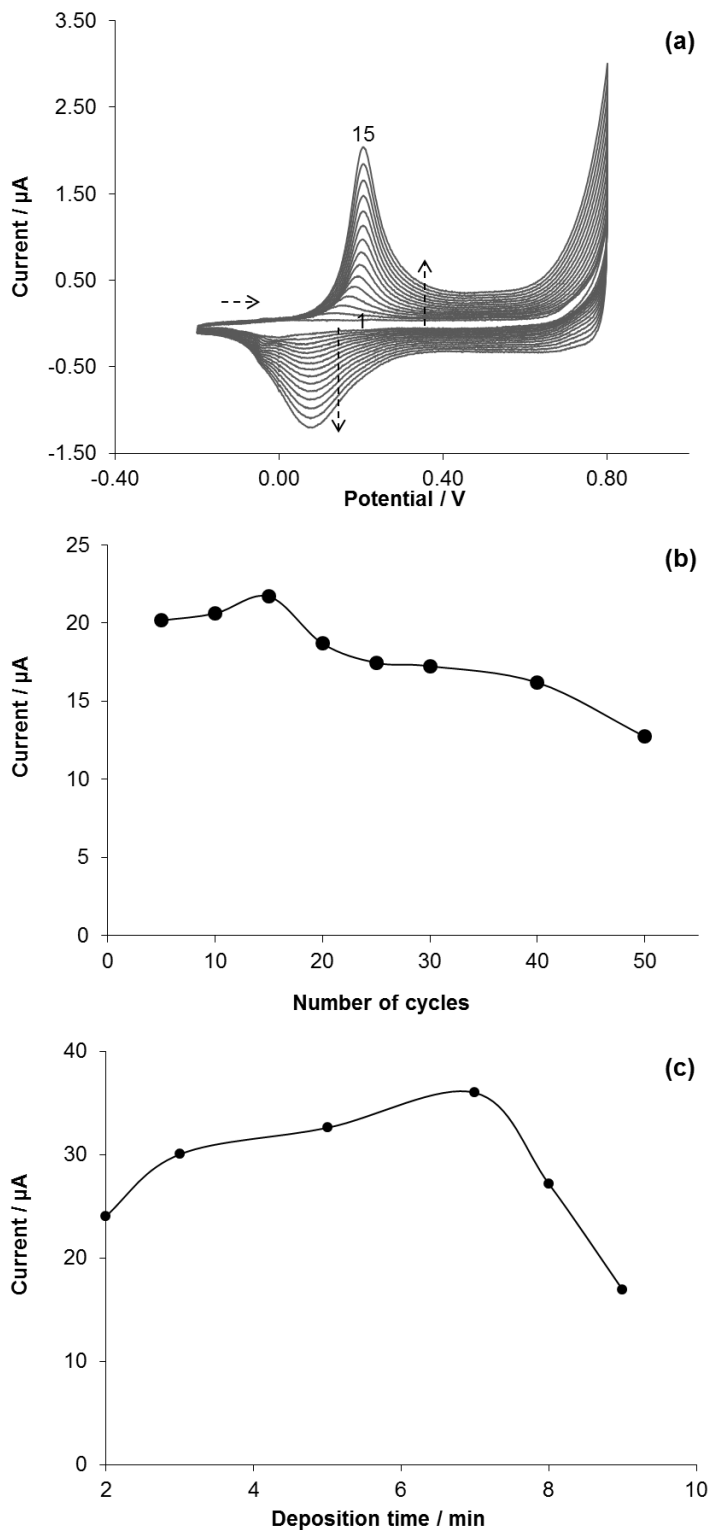


Figure 1. Electrodeposition of PANi on CPE in 1.0 M HCl + 0.10 M aniline. The number of cycles is shown in the figure (a). Current intensity of the electrooxidation of nitrite on PANi/CPE vs. number of cycles of PANi electrodeposition on the CPE (b). Current intensity of the electrooxidation of nitrite on Au/PANi/CPE vs. gold deposition time (c)

As it is seen in Figure 1b, the current response of PANi/CPE to the electrooxidation of nitrite increased when the electropolymerization cycle of PANi increased from 10 to 15 cycles, and then decreased gradually afterward. With increasing the electropolymerization cycle of PANi, the thickness of the PANi film became thicker and reached a critical thickness in which the electron transfer on the electrode is reduced. The optimum number of cycles for the electropolymerization of PANi was found to be 15 cycles (Figure 1b) as a higher response current was achieved compared to the other number of cycles. The anodic and cathodic redox peaks at 0.20 V and 0.10 V correspond to the interconversion between leucoemeraldine and emeraldine while the increase in current at approximately 0.60 V is due to the beginning of the oxidation of the second redox state of PANi, interconversion between emeraldine to pernigraniline [41]. The amount of electrodeposited PANi formed on the surface of the CPE was calculated from the height of the first oxidation peak current [42]. The optimum thickness of the deposited PANi film at 15 electropolymerization cycles was found to be 15.71 μm .

Gold was potentiostatically electrodeposited on the modified and unmodified CPE by applying a constant potential of -0.20 V at different deposition times [43]. By changing the deposition time, the amount and size of the deposited gold particles vary. The current generated in electrooxidation of nitrite on Au/PANi/CPE was evaluated at different Au deposition times (Figure 1c). At deposition times less than 7 min, the current of the electrooxidation of nitrite increased with deposition time, however, at deposition times greater than 7 min, the currents decreased gradually with further increase in deposition time. The larger deposition time of gold may result in the formation of larger gold particles. The size of the gold particles significantly influenced the catalytic efficiency. Considering the results, the optimum gold deposition time was obtained to be 7 min. The amount of gold can be calculated from the charge consumed during the electrodeposition, as reported in our previous work [44] and was found to be 21.01 μg . Undoubtedly, the more active sites available for the electrooxidation of nitrite has been achieved at the optimum parameters of 15 cycles for electropolymerization of PANi and 7 min for the electrodeposition of gold.

3.2. Characterization of Au/PANi/CPE

The morphology of the bare CPE, PANi/CPE and Au/PANi/CPE has been monitored by SEM. As Figures 2a - c show, the prepared carbon paste has been densely packed at the end of syringe tip and the gold particles have been widely distributed over the PANi/CPE. The diameter of the irregular particles was calculated from SEM images employing ImageJ software and found to be between 26 nm- 250 nm. The EDX diagram in Figure 2d shows the presence of gold and carbon from CPE (to clarify, the noisy-like narrow peaks of O and N attributed to the adsorbed oxygen and nitrogen in PANi were removed).

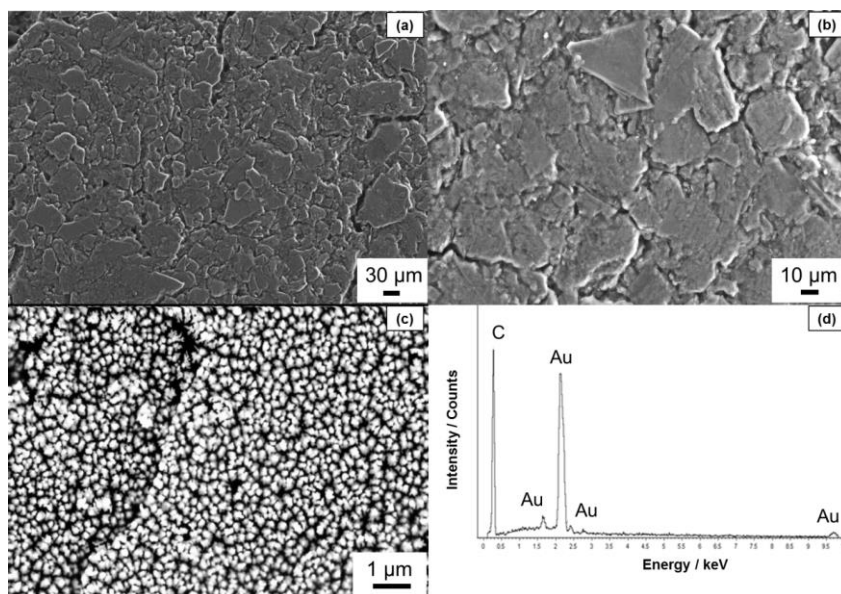


Figure 2. SEM micrographs of the bare CPE (a), PANi/CPE (b) and Au/PANI/CPE (c). EDX spectrum of Au/PANI/CPE (d)

3.3. Electrochemical Behaviour of the Prepared Electrodes

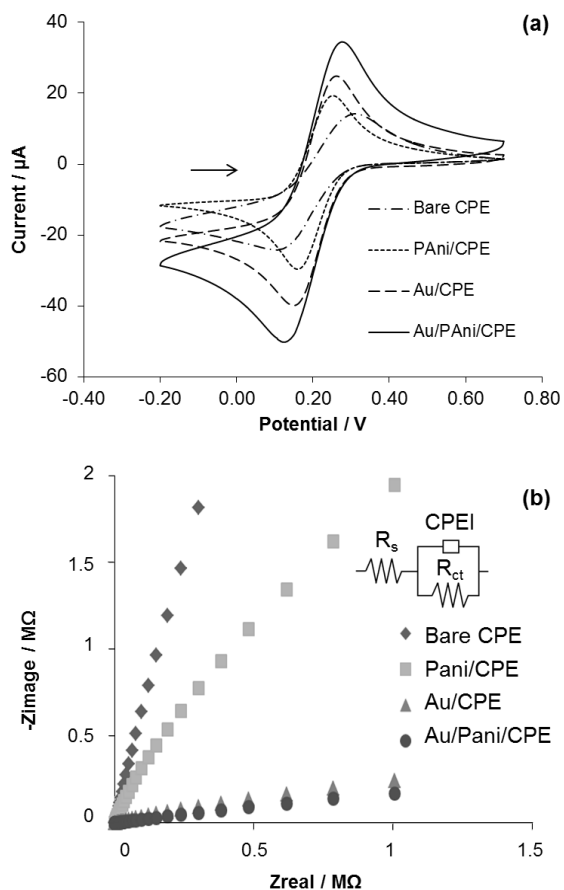


Figure 3. Cyclic voltammograms of the prepared electrodes in 0.10 M KCl containing 5 mM $K_3Fe(CN)_6/K_4Fe(CN)_6$ (a). Nyquist plots obtained for the bare CPE, PANi/CPE, Au/PANI/CPE and Au/PANI/CPE in 0.50 mM nitrite (PBS, pH 7.0) (b)

Electrochemical behaviour of the prepared CPE, PANi/CPE, Au/CPE and Au/PANi/CPE were studied by cyclic voltammetry. Figure 3a shows the cyclic voltammograms of 5 mM $K_3Fe(CN)_6/K_4Fe(CN)_6$ in 0.10 M KCl at a scan rate of 50 mV s^{-1} . As shown in the figure, the peak current increases after modification because of the increased surface area of the electrodes compared to bare CPE. The surface area of the prepared electrodes can be calculated from the Randles-Sevcik equation for the reversible system:

$$i_p = (2.69 \times 10^5) n^{3/2} A C_o D_R^{1/2} \nu^{1/2} \quad (\text{Eq. 1})$$

where i_p , n , A , C_o , D_o and ν are attributed to peak current, number of transferred electrons ($n=1$), surface area of the electrode (cm^2), concentration, diffusion coefficient ($D_R = 7.6 \times 10^{-6} \text{ cm}^2 \text{ s}^{-1}$) and scan rate (V s^{-1}), respectively. The surface area of 0.029 cm^2 , 0.036 cm^2 , 0.048 cm^2 and 0.061 cm^2 was obtained for the bare CPE, PANi/CPE, Au/CPE and Au/PANi/CPE, respectively.

The electrochemical impedance spectroscopy (EIS) experiment was employed to further study the surface properties and electrochemical behaviour of the prepared electrodes. Figure 3b shows the Nyquist plots for the various electrodes in 0.50 mM nitrite and 0.10 M phosphate buffer solution (PBS, pH 7.0). The constant phase element, CPEI (inset Figure 3b) is introduced in the equivalent circuit instead of a pure double layer capacitor to give a more accurate fit [45]. The CPEI, which is considered as the surface irregularity of the electrode, causes a greater depression in the Nyquist semi-circle where the electrode/electrolyte interface acts as a capacitor with the irregular surface [46]. The impedance of the CPEI is expressed as:

$$Z_{\text{CPEI}} = \frac{1}{Y_0(j\omega)^n} \quad (\text{Eq. 2})$$

where Y_0 is the magnitude of the CPEI, j is the imaginary unit, ω is the angular frequency ($\omega = 2\pi f$, where f is the AC frequency) and n is the CPEI exponent (phase shift). The plots are composed of semi-circles and straight-line portions, representing charge transfer and diffusion controlled processes, respectively. The R_{ct} as determined by the diameter of the semi-circle was found to be $720 \text{ } \Omega \text{ cm}^2$, $383 \text{ } \Omega \text{ cm}^2$, $213 \text{ } \Omega \text{ cm}^2$ and $111 \text{ } \Omega \text{ cm}^2$ for bare CPE, PANi/CPE, Au/CPE and Au/PANi/CPE. The R_{ct} of Au/PANi/CPE was found to be much smaller compared to other electrodes indicating that Au/PANi/CPE offers limited resistance to charge transfer in the presence of nitrite due to electronic conduction of gold, hence increasing the facilitation of charge transfer.

3.4. Electrooxidation of Nitrite on the Prepared Electrodes

As it can be seen from Figure 4a, the behaviour of CPE, PANi/CPE, Au/CPE and Au/PANi/CPE was studied in the 0.50 mM nitrite and PBS (0.10 M, pH 7.0). The wide oxidation peak at the potential of 0.80 V is attributed to oxidation of nitrite to nitrate with 2 electron transfer. The broadened peak current is because of low kinetics of electrons transfer for this reaction. A remarkable negative shift of onset potential for the electrooxidation of nitrite was observed at the Au/CPE and Au/PANi/CPE indicated faster charge transfer due to the presence of Au. The electrode modification with Au and PANi can increase the electrocatalytic performance of the Au/PANi/CPE compared to the other electrodes. This can be attributed to the high surface area and accelerated electron transfer ability of

the Au/PAni/CPE which led to the high electroactive surface for the detection of nitrite at the modified electrode.

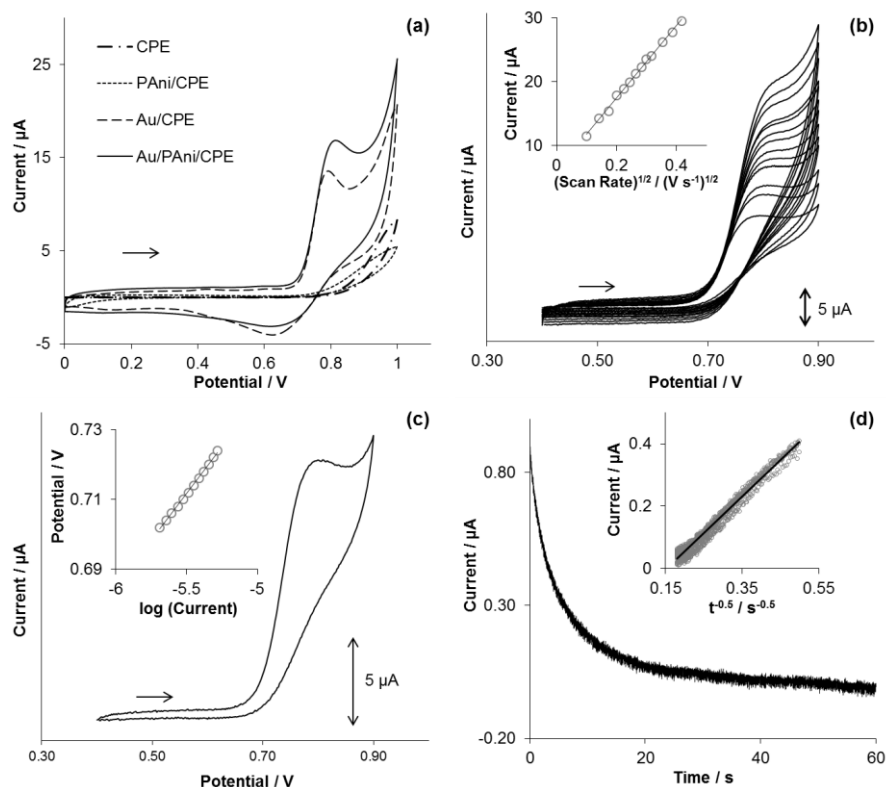


Figure 4. Electrooxidation of 0.50 mM nitrite in 0.10 M PBS (pH 7.0) (a). Cyclic voltammograms of Au/PAni/CPE in PBS (pH 7.0) containing 0.50 mM nitrite at different scan rates. Inset is the variation of the nitrite oxidation peak current versus square root of scan rate (b). Tafel plot (inset) from the rising part of the current–voltage curve at a scan rate of 20 mV s⁻¹ (c). Chronoamperometric response of the Au/PAni/CPE in 0.40 mM nitrite in 0.10 M PBS (pH 7.0). Inset is current versus square root of time derived from the chronoamperogram (d)

3.4.1. Effect of scan rate

Effect of scan rate on the electrochemical oxidation of nitrite has been studied. Figure 4b shows the cyclic voltammograms of Au/PAni/CPE in 0.50 mM nitrite and 0.10 M PBS, pH 7.0 at different scan rates. As the scan rate increases, the peak current of the nitrite electrooxidation proportionally increases with square root of scan rate with the best fit between 10 mV s⁻¹ and 175 mV s⁻¹. The equation indicates that the current of nitrite electrooxidation at Au/PAni/CPE in the mentioned potential window is linear against the square root of scan rate (inset) and follows form equation as i_p (μA) = 56.52 $v^{1/2}$ (V^{1/2}s^{-1/2}) + 6.16 (R² = 0.997). The equation with non-zero intercept indicates that the electrooxidation of nitrite over Au/PAni/CPE is not a fully diffusion-controlled process.

To calculate the kinetic parameters, the Tafel plot of potential versus logarithm of current was plotted from the rising part of current–potential curve for the oxidation of nitrite at a scan rate of 0.020 V s⁻¹ (Figure 4c). The Tafel slope value was found to be 0.053 V/decade (inset) which indicates that

the rate-determining step is a chemical reaction with one-electron transfer process. $(1-\alpha)n_\alpha$ was calculated to be 0.69 at the Au/PAni/CPE electrode using equation bellow:

$$(1 - \alpha)n_\alpha = 0.477(V)/(E_p - E_{p/2}) \tag{Eq. 3}$$

where α , n_α , E_p and $E_{p/2}$ are transfer coefficient, number of electrons in the rate determining step, peak potential and half-wave potential, respectively.

3.4.2. Determination of diffusion coefficient

To determine the diffusion coefficient of nitrite in the PBS (pH 7.0), the chronoamperometric experiment was employed by applying a constant potential of 0.80 V to Au/PAni/CPE for 60 s (Figure 4d). According to the Cottrell equation, the Cottrellian behaviour of the Au/PAni/CPE can be seen by plotting the current against 1/square root of time (inset):

$$i = \frac{nFA D_o^{1/2} C_o}{\pi^{1/2} t^{1/2}} \tag{Eq. 4}$$

where A , D_o , C_o and t are the electrode surface area (cm^2), diffusion coefficient ($\text{cm}^2 \text{s}^{-1}$), concentration (mol cm^{-3}) and time (s), respectively. The i vs. $t^{-1/2}$ of the Au/PAni/CPE in $0.040 \mu\text{M} + 0.10 \text{ M}$ PBS (pH 7.0) was plotted. From the slope of i vs. $t^{-1/2}$, the diffusion coefficient can be determined according to Equation 4. The value of the diffusion coefficient was found to be $1.93 \times 10^{-5} \text{ cm}^2 \text{ s}^{-1}$ which is close to formerly reported values [36, 47].

3.4.3. Effect of temperature

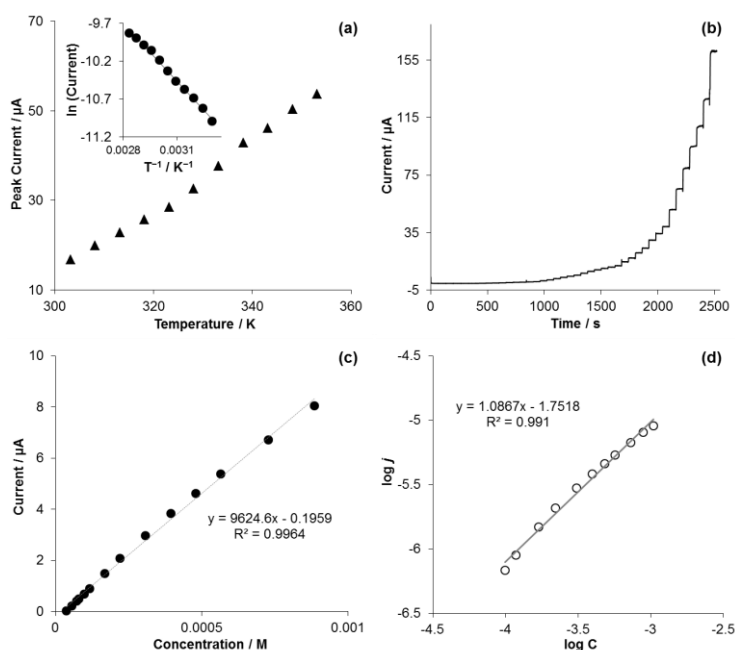


Figure 5. The electrooxidation of 0.50 mM nitrite in 0.10 M PBS (pH 7.0) at Au/PAni/CPE at different temperatures (Inset. $\ln i$ was plotted versus $1/T$) (a). Amperograms of nitrite at Au/PAni/CPE in PBS (pH 7.0) with successive addition of nitrite (b). Electrooxidation current of 0.50 mM nitrite in 0.10 M PBS (pH 7.0) vs. the concentration of nitrite (c). Logarithm of current vs. logarithm of concentration of nitrite (d)

The electrooxidation of 0.50 mM nitrite in 0.10 M PBS (pH 7.0) at Au/PAni/CPE has been studied at different temperatures by cyclic voltammetry. Figure 5a indicates that the electrooxidation of nitrite is a temperature-dependent process. As the medium temperature increases, the peak current of the electrooxidation of nitrite increases which is due to acceleration in electron transfer at the electrolyte-electrode interface. To calculate the apparent activation energy (E_a), the values of $\ln i$ was plotted versus $1/T$ (inset) obtained from the equation below:

$$\ln i = \ln i_0 - \frac{E_a}{RT} \quad (\text{Eq. 5})$$

where i , R and T are the current, universal constant of gases ($8.314 \text{ J mol}^{-1} \text{ K}^{-1}$) and temperature (K). The plot gives a straight line which the activation energy can be calculated from the slope. The value for E_a was found to be ca. 21.0 kJ mol^{-1} . The electrooxidation of nitrite on the Au/PAni/CPE is less than the reported value on the PAni-Cu nanocomposit modified glassy carbon electrode (GCE) [37].

3.4.4. Effect of concentration

To determine the linear range for nitrite detection on Au/PAni/CPE, the chronoamperometry technique was employed in 0.10 M PBS containing different concentrations of nitrite (Figure 5b). The amperogram response to the successive addition of nitrite in 60 s intervals in hydrodynamic condition (stirring solution at 1200 rpm) was recorded at the constant potential of 0.80 V. The current linearly increases by increasing the concentration of nitrite between $3.8 \times 10^{-5} \text{ M}$ to $1.0 \times 10^{-3} \text{ M}$ (Figure 5c) with a detection limit of $2.5 \times 10^{-5} \text{ M}$ ($S/N = 3$) and sensitivity of 0.0093 A/M . For comparison, the electrocatalytic performance of other reported gold catalysts has been tabulated in Table 1.

The order of reaction of the electrooxidation of nitrite in PBS (pH 7.0) on the Au/PAni/CPE can be determined. As $j = j_0[\text{NO}_2^-]^n$, the order of this reaction can be calculated from the slope of $\log j$ versus $\log [\text{NO}_2^-]$ in the Figure 5d. The order of electrooxidation of nitrite in PBS (pH 7.0) was found to be 1.09 which shows the electrooxidation of nitrite on Au/PAni/CPE follows first order kinetics.

Table 1. Linear concentration range (C) and limit of detection (LOD) of the electrodes for determination of nitrite. Db: 1-azonia-4-azabicyclo, FTO: fluorine-doped tin oxide

Electrode	C (M)	LOD (M)	Medium	Reference
Au ultramicroelectrode	$1.0 \times 10^{-4} - 6.0 \times 10^{-4}$	6.5×10^{-4}	Na_2SO_4	[48]
Nano Au/GCE	$1.3 \times 10^{-4} - 4.4 \times 10^{-2}$	4.5×10^{-5}	PBS pH 5.0	[49]
Nanoporous Au leaf	$1.0 \times 10^{-6} - 1.0 \times 10^{-3}$	1.0×10^{-6}	PBS pH 4.5	[50]
single-layer graphene nanoplatelet-protein composite film	$5.0 \times 10^{-5} - 2.5 \times 10^{-3}$	1.0×10^{-5}	PBS pH 5.0	[51]
poly-[Ru(5-NO ₂ -phen) ₂ Cl] tetrapyrrolylporphyrin/GCE	$1.5 \times 10^{-5} - 1.2 \times 10^{-4}$	9.4×10^{-6}	NaClO_4 pH 5.9	[52]
Au-Py/AlSi	$7.9 \times 10^{-5} - 7.4 \times 10^{-4}$	1.3×10^{-6}	Britton-Robinson	[53]
Au-Db/AlSi		3.0×10^{-6}	Buffer pH 7.3	
Au/FTO	$1.0 \times 10^{-5} - 7.5 \times 10^{-4}$	2.9×10^{-6}	PBS pH 7.0	[54]
AuNPs/mesoporous carbon	$5.0 \times 10^{-6} - 7.2 \times 10^{-3}$	4.2×10^{-7}	PBS pH 6.5	[55]
Nanoporous PdFe	$5.0 \times 10^{-4} - 2.6 \times 10^{-2}$	0.8×10^{-6}	PBS pH 7.0	[56]
Au/PAni/CPE	$3.8 \times 10^{-5} - 1.0 \times 10^{-3}$	2.5×10^{-5}	PBS pH 7.0	This work

3.4.5. Effect of Interferences

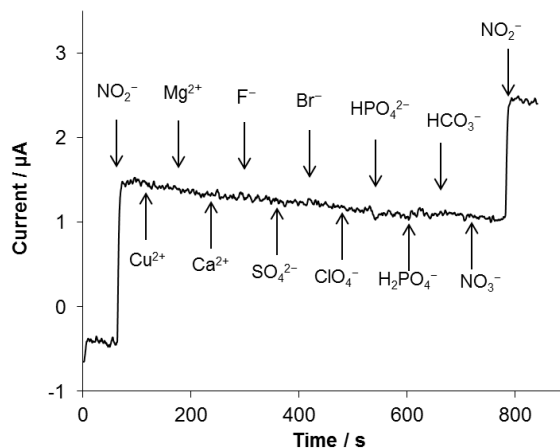


Figure 6. Amperometric responses at Au/PAni/CPE to successive additions of the interferences in presence of 1.0 mM nitrite and PBS pH 7.0 at 0.80 V in hydrodynamic conditions

Figure 6 shows the effect of different ions as the interferences on the electrooxidation of nitrite by chronoamperometry. The performance of the Au/PAni/CPE was studied in 0.50 mM nitrite in PBS (pH 7.0) containing 50-fold concentration of Cu^{2+} , Mg^{2+} , Ca^{2+} , F^- , SO_4^{2-} , Br^- , ClO_4^- , HPO_4^{2-} , H_2PO_4^- , HCO_3^- , and NO_3^- ions. As can be seen in Figure 6, the Au/PAni/CPE is selective to nitrite ions in the presence of the mentioned interfering ions.

3.4.6. Stability, reproducibility and repeatability

To evaluate the repeatability of the sensor, electrochemical experiments were repeatedly carried out by comparing the CVs peak current response to 1.0 mM nitrite at five Au/PAni/CPEs independently. The sensors exhibited appreciable relative standard deviation (RSD) of 3.52% for the determination of nitrite, which revealed that the modified electrode displayed an acceptable repeatability. The reproducibility of the sensor was measured by using one independent electrode for 5 samples of 1.0 mM nitrite. The RSD was found to be 2.39% which indicated excellent reproducibility. The stability of the electrode was examined by measuring the alteration in responses to 1.0 mM nitrite in 0.10 M PBS (pH 7.0) after a period of time of 1 month. Only 11% decrease in peak current after a month suggesting good stability of the modified electrode.

3.4.7. Determination of nitrite ions in real samples

The practical application of the Au/PAni/CPE was determined by measuring the concentration of nitrite ions present in the water samples collected from rain, tap water and lake water (USM Lake, Penang, Malaysia). The standard addition technique was used for the determination of nitrite ions in water samples ($n = 5$). The results are summarized in Table 2.

Table 2 The recovery determination of nitrite in real samples ($n = 5$)

Sample	Original	Added (μM)	Found (μM)	Recovery
Rain	-	80.0	81.3	102%
Tap water	-	80.0	79.0	98.7%
Lake water	-	80.0	80.3	100%

All samples were filtered before analysis. The results are given in the Table 2 which shows a good recovery between 98.7% and 102% at Au/PAni/CPE for the water samples spiked with nitrite

4. CONCLUSIONS

The gold particles/ polyaniline modified carbon paste electrode (Au/PAni/CPE) was prepared to study the electrooxidation of nitrite ions. The Au/PAni/CPE showed a good electrocatalytic performance towards the electrooxidation of nitrite compared to Au/CPE, PAni/CPE and bare CPE. The Au/PAni/CPE had a larger surface area compared to the other electrodes with an appropriate concentration range and detection limit for the electrooxidation of nitrite. The oxidation current response at the Au/PAni/CPE was found to be linearly proportional to the nitrite concentration in the range of 3.8×10^{-5} M to 1.0×10^{-3} M with a detection limit of 2.5×10^{-5} M ($S/N = 3$). The Au/PAni/CPE was applied for the determination of nitrite in real water samples. The electrode was also found to exhibit a desirable stability, repeatability and selectivity.

ACKNOWLEDGEMENTS

This work which has been carried out at Universiti Sains Malaysia (USM)- has been supported by a RU-Grant (1001/ PKIMIA/ 811056) from USM

References

1. L. J. Dombrowski and E. J. Pratt, *Anal. Chem.*, 44 (1972) 2268
2. E. García-Robledo, A. Corzo and S. Papaspyrou, *Mar. Chem.*, 162 (2014) 30
3. B. Schnetger and C. Lehnert, *Mar. Chem.*, 160 (2014) 91
4. K. M. Miranda, M. G. Espey and D. A. Wink, *Nitric Oxide*, 5 (2001) 62
5. S. B. Butt, M. Riaz and M. Z. Iqbal, *Talanta*, 55 (2001) 789
6. N. Wang, R. Q. Wang and Y. Zhu, *J. Hazard. Mater.*, 235-236 (2012) 123
7. A. Büldt and U. Karst, *Anal. Chem.*, 71 (1999) 3003
8. A. Wu, T. Duan, D. Tang, Y. Xu, L. Feng, Z. Zheng, J. Zhu, R. Wang and Q. Zhu, *Chromatographia*, 76 (2013) 1649
9. M. Akyüz and Ş. Ata, *Talanta*, 79 (2009) 900
10. X. Wang, E. Masschelein, P. Hespel, E. Adams and A. V. Schepdael, *Electrophoresis*, 33 (2012) 402
11. Y. Zhang, X. Tian, Y. Guo, H. Li, A. Yu, Z. Deng, B. B. Sun and S. Zhang, *J. Agric. Food.*

- Chem.*, 62 (2014) 3400
12. V. Mani, A. P. Periasamy and S.-M. Chen, *Electrochem. Commun.*, 17 (2012) 75
 13. B. Unnikrishnan, P.-L. Ru, S.-M. Chen and V. Mani, *Sens. Actuat. B*, 177 (2013) 887
 14. B. R. Kozub, N. V. Rees and R. G. Compton, *Sens. Actuat. B*, 143 (2010) 539
 15. L. Jiang, R. Wang, X. Li, L. Jianga and G. Lu, *Electrochem. Commun.*, 7 (2005) 597
 16. W. S. Cardoso and Y. Gushikem, *J. Electroanal. Chem.*, 583 (2005) 300
 17. M. H. Pournaghi-Azar and H. Dastango, *J. Electroanal. Chem.*, 567 (2004) 211
 18. C. A. Caro, F. Bedioui and J. H. Zagal, *Electrochim. Acta*, 47 (2002) 1489
 19. N. Spătaru, T. N. Rao, D. A. Tryk and A. Fujishima, *J. Electrochem. Soc.*, 148 (2001) E112
 20. X.-H. Pham, C. A. Li, K. N. Han, B.-C. Huynh-Nguyen, T.-H. Le, E. Ko, J. H. Kim and G. H. Seong, *Sens. Actuat. B*, 193 (2014) 815
 21. Z. Wang, F. Liao, T. Guo, S. Yang and C. Zeng, *J. Electroanal. Chem.*, 664 (2012) 135
 22. R. Guidelli, F. Pergola and G. Raspi, *Anal. Chem.*, 44 (1972) 745
 23. M. Etesami and N. Mohamed, *J. Anal. Chem.*, 71 (2016) 185
 24. X. Xing and D. A. Scherson, *Anal. Chem.*, 60 (1988) 1468
 25. S. Sunohara, K. Nishimura, K. Yahikozawa, M. Ueno, M. Enyo and Y. Takasu, *J. Electroanal. Chem.*, 354 (1993) 161
 26. L. Agüí, C. Peña-Farfal, P. Yáñez-Sedeño and J. M. Pingarrón, *Talanta*, 74 (2007) 412
 27. A. Afkhami and H. Ghaedi, *Analytical Methods*, 4 (2012) 1415
 28. A. Afkhami, F. Soltani-Felehgari and T. Madrakian, *Electrochim. Acta*, 103 (2013) 125
 29. J. Raouf, R. Ojani and M. Ramine, *J. Solid State Electrochem.*, 13 (2009) 1311
 30. R. Ojani, J.-B. Raouf and B. Norouzi, *Electroanalysis*, 20 (2008) 1996
 31. S.-J. Li, G.-Y. Zhao, R.-X. Zhang, Y.-L. Hou, L. Liu and H. Pang, *Microchim. Acta*, 180 (2013) 821
 32. A.-J. Lin, Y. Wen, L.-J. Zhang, B. Lu, Y. Li, Y.-Z. Jiao and H.-F. Yang, *Electrochim. Acta*, 56 (2011) 1030
 33. T.-S. Liu, T.-F. Kang, L.-P. Lu, Y. Zhang and S.-Y. Cheng, *J. Electroanal. Chem.*, 632 (2009) 197
 34. X. Huang, Y. Li, Y. Chen and L. Wang, *Sens. Actuat. B*, 134 (2008) 780
 35. Y. Cui, C. Yang, W. Zeng, M. Oyama, W. Pu and J. Zhang, *Anal. Sci.*, 23 (2007) 1421
 36. J. Li, *Chin. J. Chem.*, 27 (2009) 2373
 37. Y. Zhang, J. Yin, K. Wang, P. Chen and L. Ji, *J. Appl. Polym. Sci.*, 128 (2013) 2971
 38. A. I. Gopalan, K.-P. Leea and S. Komathi, *Biosens. Bioelectron.*, 26 (2010) 1638
 39. M. Trojanowicz, *Microchim. Acta*, 143 (2003) 75
 40. M. J. Croissant, T. Napporn, J. M. Léger and C. Lamy, *Electrochim. Acta*, 43 (1998) 2447
 41. A. M. Bonastre and P. N. Bartlett, *Anal. Chim. Acta*, 676 (2010) 1
 42. L. Wang, C. Chen, Y. Fu, Q. Xie, Z. Su, C. Qin, F. Xie, M. Ma and S. Yao, *Electroanalysis*, 23 (2011) 1681
 43. M. Etesami and N. Mohamed, *J. Chin. Chem. Soc.*, 61 (2014) 377
 44. M. Etesami and N. Mohamed, *Chemija*, 23 (2012) 171
 45. E. A. Noor and A. H. Al-Moubaraki, *Mater. Chem. Phys.*, 110 (2008) 145
 46. A. K. Satapathy, G. Gunasekaran, S. C. Sahoo, K. Amit and P. V. Rodrigues, *Corros. Sci.*, 51 (2009) 2848
 47. A. Afkhami, F. Soltani-Felehgari, T. Madrakian and H. Ghaedi, *Biosens. Bioelectron.*, 51 (2014) 379
 48. S. M. da Silva and L. H. Mazo, *Electroanalysis*, 10 (1998) 1200
 49. Y. Liu and H.-Y. Gu, *Microchim. Acta*, 162 (2008) 101
 50. X. Ge, L. Wang, Z. Liu and Y. Ding, *Electroanalysis*, 23 (2011) 381
 51. R. Yue, Q. Lu and Y. Zhou, *Biosens. Bioelectron.*, 26 (2011) 4436
 52. P. Dreyse, M. Isaacs, K. Calfumán, C. Cáceres, A. Aliaga, M. J. Aguirre and D. Villagra,

- Electrochim. Acta*, 56 (2011) 5230
53. E. de Menezes, M. Nunes, L. Arenas, S. P. Dias, I. S. Garcia, Y. Gushikem, T. H. Costa and E. Benvenutti, *J. Solid State Electrochem.*, 16 (2012) 3703
54. M. M. Rahman, X. B. Li, N. S. Lopa and J. J. Lee, *Bull. Korean Chem. Soc.*, 35 (2014) 2072
55. X. J. Yang, Y. H. Wang, J. Bai, X. Y. He and X. E. Jiang, *RSC Advances*, 5 (2015) 2956
56. J. Wang, H. Zhou, D. Fan, D. Zhao and C. Xu, *Microchim. Acta*, 182 (2015) 1055

© 2016 The Authors. Published by ESG (www.electrochemsci.org). This article is an open access article distributed under the terms and conditions of the Creative Commons Attribution license (<http://creativecommons.org/licenses/by/4.0/>).